Author(s): Lee, Young Joo & von Boehm, J. & Pesola, M. & Nieminen, Risto M.

Title: Aggregation Kinetics of Thermal Double Donors in Silicon

Year: 2001

Version: Final published version

Please cite the original version:

Lee, Young Joo & von Boehm, J. & Pesola, M. & Nieminen, Risto M. 2001. Aggregation Kinetics of Thermal Double Donors in Silicon. Physical Review Letters. Volume 86, Issue 14. 3060-3063. ISSN 0031-9007 (printed). DOI: 10.1103/physrevlett.86.3060.

Aggregation Kinetics of Thermal Double Donors in Silicon

Young Joo Lee, J. von Boehm, M. Pesola, and R. M. Nieminen
COMP/Laboratory of Physics, Helsinki University of Technology, P.O. Box 1100, FIN-02015 HUT, Finland
(Received 21 August 2000)

A general kinetic model based on accurate density-functional-theoretic total-energy calculations is introduced to describe the aggregation kinetics of oxygen-related thermal double donors (TDD's) in silicon. The calculated kinetics, which incorporates the reactions of associations, dissociations, and isomerizations of all relevant oxygen complexes, is in agreement with experimental annealing studies. The aggregation of TDD's takes place through parallel-consecutive reactions where both mobile oxygen dimers and fast migrating chainlike TDD's capture interstitial oxygen atoms.

DOI: 10.1103/PhysRevLett.86.3060 PACS numbers: 61.72.Bb, 61.72.Cc, 61.72.Tt

Aggregation of supersaturated oxygen in as-grown Czochralski silicon occurs in the temperature range 350–550 °C via a fast diffusion (FD) mechanism, resulting in a family of electrically active complexes called thermal double donors (TDD's) [1,2]. FD has a considerably lower activation energy (by ~0.8 eV) compared to that of normal interstitial oxygen (O_i) hopping diffusion. The mechanism of this technologically important and scientifically challenging phenomenon has remained obscure [1].

Combined infrared (IR) spectroscopy and resistivity measurements are commonly used in studying the clustering of oxygen and the TDD formation kinetics [3]. The IR bands at 975, 988, 999, and 1013 cm^{-1} are assigned to TDD1, TDD2, TDD3, and staggered oxygen dimer, respectively [3–6], while the 1005 cm^{-1} band has been variably interpreted as a TDD $\geq$ TDD4 [4], oxygen dimer (O_2) [7], or oxygen trimer (O_3) [8]. The TDD formation is found to take place in two stages: The first stage mainly due to the formation of the 975 cm^{-1} band with a low activation energy of 1.2 eV [9] and the second stage due to the later TDD's with an activation energy of 1.7–1.8 eV [9–12].

A popular model for FD is one where only O_2's act as the FD species [1]. In this model there is a common core to which O_2's aggregate to form a series of closely related TDD's. However, problems arise in having only O_2 as a FD species because extremely high values of O_2 diffusivity are required to account for the successive transformations of the first TDD's [8]. To circumvent this problem Murin and Markevich [8] suggest that also O_3's must act as FD species. However, Åberg *et al.* [5] conclude that the O_3 formation rate would be 3 orders of magnitude larger than any other reaction rate of O_2 and exclude this possibility in their kinetic model. Götz *et al.* [13] present a kinetic model for the formation and annihilation of TDD's at 550 °C without the assumption of FD of oxygen at all. In this Letter we introduce a general kinetic model and show that *not only* O_2's but *also* O_3's *and* TDD's *themselves act as* FD species. We find that the growth of TDD's takes place through diffusion-limited reactions where first migrating O_2's, and then fast migrating O_3's and TDD's, *capture* O_i's, i.e., TDDn + $O_i \rightarrow$ TDD(n + 1).

Our kinetic model is based on the results for the energetics of isomers, activation energies of migration and isomerization, and binding energies of oxygen complexes by the density-functional-theory calculations within the local density approximation for exchange-correlation energy. Using the calculated total energies we have been able [14] to identify oxygen chainlike structures — consisting of one or more four-member rings (R) and flanking O_i's — as the donors assigned the symbols TDD0, . . . , TDD7 in the primary TDD family. The R unit consists of two threefold coordinated O atoms bonded to two common Si atoms [15].

The calculations have been performed using the plane-wave pseudopotential (PP) techniques (FINGER code) [16]. For oxygen, the ultrasoft Vanderbilt [17] PP is used; for silicon, the norm-conserving [18] PP with nonlinear core-valence corrections is applied. The kinetic energy cutoff was 28 Ry, and large, elongated supercells with up to 162 atoms were used, with the Γ point sampling in the reciprocal space. The structures were obtained by allowing all ionic coordinates to relax without any constraints until the largest remaining Hellmann-Feynman force component was less than 1 meV/Å. The migration paths and barriers used in our kinetic model were obtained by moving the O complexes as follows [19]. A chosen (but arbitrary) atom (O or Si) of the oxygen complex was bound to move in the plane perpendicular to the jump-defining vector connecting its initial and final positions [19]. All the other atoms were allowed to relax without constraints. The plane was moved in steps of 0.1 Å.

The kinetic model includes the dissociation and isomerization reactions of oxygen complexes as well as the association reactions mediated by diffusion. The association of two migrating oxygen complexes O_j (containing j O atoms) and O_k into an O_{j+k} complex occurs with the reaction rate $(1 + \delta_{jk})^{-1} 4\pi r_0 (D_j + D_k)[O_j][O_k]$, where r_0 is the capture radius for the reaction (set to a typical value of 5 Å throughout), $D_j = D_{j0} \exp(-E_j^m/kT)$ is the diffusivity of the O_j (D_{j0} is the preexponential factor and E_j^m is the migration energy), and $[O_j]$ is the concentration of the O_j [20]. The oxygen complex may be a straight chain or a complex of a more general shape. The calculated migration energies for the latter are much higher

 0031-9007/01/86(14)/3060(4)$15.00

than for the straight chains (typically by about 1.5–2.0 eV) so that practically all migration is mediated by straight chains along the $[1\bar{1}0]$ directions. The dissociation of the O_{j+k} complex into O_j and O_k occurs with the reaction rate $Ar_0^{-2}(D_j + D_k)\exp(-E_{jk}^b/kT)[O_{j+k}]$ where A is a dimensionless factor and E_{jk}^b is the binding energy of O_{j+k} against dissociation into O_j and O_k. Also, since the formation energies of the straight chains are lower than those of the less symmetric complexes, substantial isomerization of the latter into the straight chains occurs. The isomerization rate is $\nu\exp(-\Delta E_a/kT)[O_k]$, where ν is a frequency factor and ΔE_a is the activation energy.

We use for the factor AD_{j0}/r_0^2 the value of 0.4717×10^{15} s^{-1} for processes where O_i is ejected from the complex [21]. In all other dissociation and restructuring cases, the common value 0.8772×10^{12} s^{-1} is used for the prefactor [21]. For the diffusivity of O_i we use the experimental preexponential factor of 0.17 cm^2 s^{-1} [21]. The preexponential factors for the diffusivities of the O_2, O_3, and O_4 chains are obtained by fitting the calculated concentration of staggered O_2 to the experimental concentration of the 1013 cm^{-1} band at 350 and 420 °C [Figs. 1(a) and 1(d) of Ref. [5]].

As an example of diffusion, Fig. 1 shows the migration mechanism of the O_4 chain along a $[1\bar{1}0]$ direction. The initial configuration shown in Fig. 1(a) is the electrically inactive staggered structure [14,22]. The migration starts by forming one R at the right end (the O atoms belonging to R are denoted by O_r). The complex becomes electrically active due to the two threefold coordinated O_r atoms. The corresponding stable O_{2i}-O_{2r} structure shown in Fig. 1(b) is assigned to TDD1 [14]. In the next stage a second adjacent R is formed in the middle of the O_4 chain [Fig. 1(c)]. This structure is, in fact, unstable but turns out to be the core for the later complexes assigned to TDD3–TDD7. In the next stage only the R in the middle of the O_4 chain persists. This O_i-O_{2r}-O_i structure, shown in Fig. 1(d), is assigned to TDD2 [14]. Next, two R's are formed to the left end leading to the O_{2r}-O_{2i} structure (TDD1). Finally the staggered structure is recovered. To continue the migration, the rotation of the four O_i's by 180° around their Si-Si lines over small barriers (the calculated rotational barriers are 0.1 eV for isolated staggered O_2) is needed.

Figure 1(e) shows the variation of the calculated lowest transformation energy in n- and p-type silicon. The energies are calculated for three possible charge states (neutral, singly, doubly positive), and Figs. 1 and 2 show the lowest values. The charge states change from neutral to doubly positive and back to neutral as the reaction coordinate changes from 0 to 1. The net migration energies are lowered for all oxygen complexes ($n \geq 2$) due to the charge-exchange mechanism [23]. Figure 1(e) also displays the

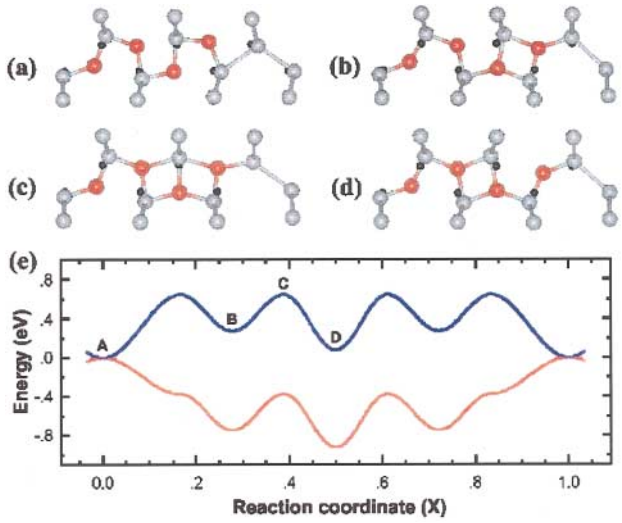

FIG. 1 (color). Diffusion mechanism of O_4 chain along the $[1\bar{1}0]$ direction. (a) Staggered O_4. (b) O_{2i}-O_{2r} (TDD1). (c) The structure of O_4 at the reconfiguration barrier C. (d) O_i-O_{2r}-O_i (TDD2). (e) The total (formation) energy of the O_4 chain. A, B, C, and D correspond to the structures of (a), (b), (c), and (d), respectively. The upper (lower) curve is calculated with the electron chemical potential $\mu_e = 0.55$ (0.0) eV. The red and blue balls denote the oxygen and silicon atoms, respectively. Black dots show the lattice points of the perfect silicon crystal in equilibrium state.

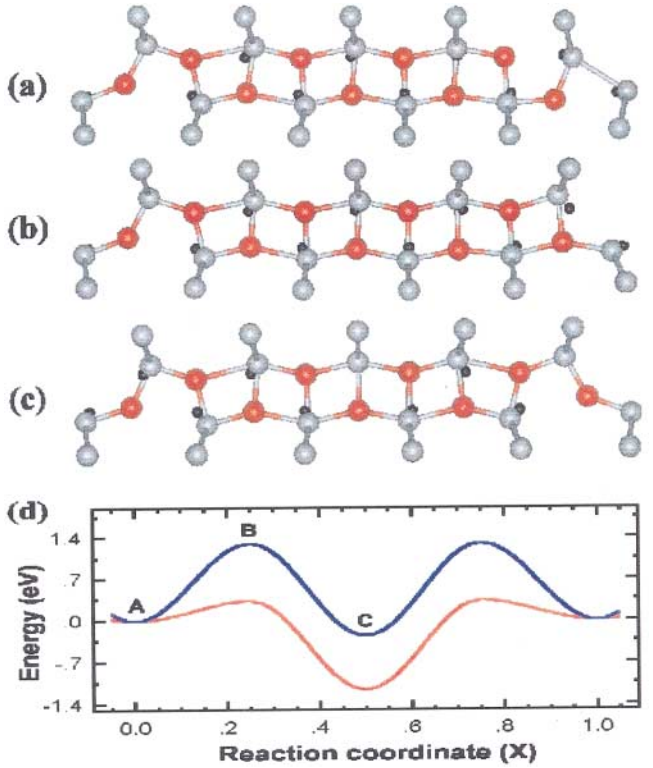

FIG. 2 (color). Diffusion mechanism of O_9 chain along the $[1\bar{1}0]$ direction. (a) Electrically inactive O_i-O_{7r}-O_i structure. (b) O_i-O_{8r}. (c) C_{2v}-symmetric O_i-O_{7r}-O_i structure (TDD7). (d) The total (formation) energy of the O_9 chain. A, B, and C correspond to the structures of (a), (b), and (c), respectively. The upper (lower) curve is calculated with the electron chemical potential $\mu_e = 0.55$ (0.0) eV.

bistability found experimentally for TDD1 and TDD2 in n-type silicon [2,24,25] as well as the O_{2i}-$O_{2r} \rightarrow O_i$-O_{2r}-O_i reconfiguration suggested by the experimental kinetic study for TDD1 $\rightarrow$ TDD2 [5].

The O_3 chain migrates in the same way: First starting with a staggered O_3 one R is formed at the right end. This O_i-O_{2r} structure is assigned to TDD0 [14]. Then the O_{2r}-O_i structure is formed via the R_2 structure, and finally the staggered O_3 is recovered. The oxygen dimer O_2 is found to migrate via forming one R in agreement with Ref. [15].

As another example, Fig. 2 shows the migration mechanism of the O_9 chain along the $[1\bar{1}0]$ direction. Starting from the electrically inactive O_i-O_{7r}-O_i structure of Fig. 2(a) first one R is formed at its right end as is shown in Fig. 2(b). Then the electrically active (nearly) C_{2v} symmetric O_i-O_{7r}-O_i structure of Fig. 2(c)—assigned to TDD7 [14]—is formed by breaking the lower Si-O_r bond of the rightmost R. The step continues via the formation of one R at the left end. To continue the migration, the rotation of the four O_i's by 180° around their Si-Si lines is needed. The rotational part may cost here more energy than in the case of the O_4 chain due to adjacent R's. However, it is expected (and here assumed) that the rotation barrier does not exceed the migration energy determined by the calculated total energy shown in Fig. 2(d). The single deep minimum for the C_{2v} symmetric O_i-O_{7r}-O_i structure in the middle of Fig. 2(d) reflects the fact that the bistability has disappeared. The bistability does not appear in the $O_5, \ldots, O_8$ chains either because they also have a similar single deep minimum (the corresponding structures being assigned to TDD3, ..., TDD6 [14]). This behavior agrees with experiments [2,24,25]. Figure 3 shows the calculated migration energies of the studied R chains as a function of the electron chemical potential μ_e. It is noticeable that the O_3, O_4, and O_5 chains have lower migration energies than O_2 in n-type silicon.

The kinetics of the oxygen complexes is then simulated by solving the coupled kinetic equations consisting of associations, dissociations, and isomerizations with the activation energies obtained from first principles calculations. Figure 4 shows the simulated annealing behavior of the first oxygen chains in n-type silicon at 420 °C. We find that the behaviors of the simulated concentrations of staggered O_3, O_{2i}-O_{2r} (TDD1), O_i-O_{2r}-O_i (TDD2), and O_i-O_{3r}-O_i (TDD3) agree closely with those of the respective experimental 1005, 975, 988, and 999 cm^{-1} bands by Åberg *et al.* [5]. Also the results for other annealing temperatures agree closely with the experimental results by Åberg *et al.* [5]. The experimental concentration of the oxygen complex corresponding to the 1005 cm^{-1} IR band is quite close to the simulated concentration of O_3 rather than that of TDD's $\geq$ TDD4 suggested in Ref. [5]. Åberg *et al.* also speculated the association reaction of O_i and O_2 for the O_3 clusters, and find that according to a simple diffusion-limited reaction a large amount of O_3 should be observed. However, such high concentrations of O_3 are not observed. Åberg *et al.* have not taken into account the diffusivity of O_3 clusters. If the migration of O_3 is included in the kinetics, the O_3 formed by the association reaction of O_2 and O_i is balanced by the association reaction of O_3 and O_i. We find that the aggregation process of TDD's is of the parallel-consecutive reaction type: All oxygen chains act as FD species and *capture* slowly moving O_i's. We can assign the 1005 cm^{-1} band to the staggered O_3 (see Fig. 4) in agreement with Ref. [8]. We also avoid the anomalously high diffusivity of O_2 which is usually a consequence of the assumption that *only* O_2's act as a FD

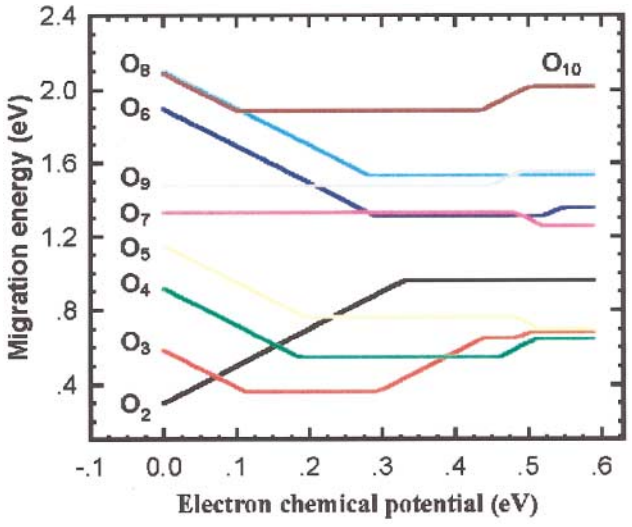

FIG. 3 (color). Calculated migration energies as a function of the electron chemical potential μ_e. O_n denotes a chain with n oxygen atoms.

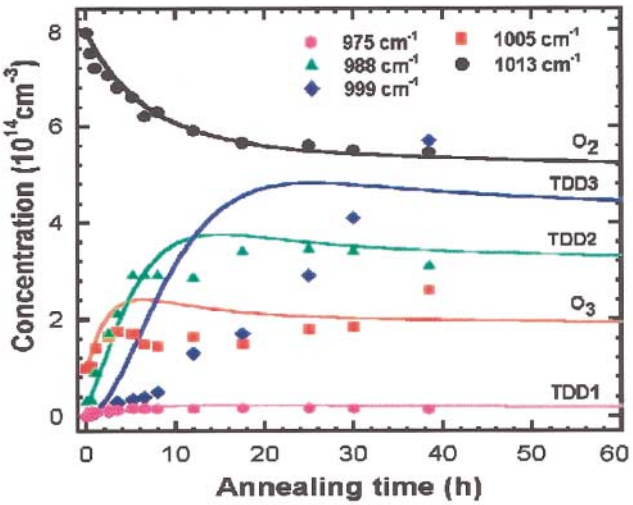

FIG. 4 (color). Simulated annealing behavior of the first oxygen chains in n-type silicon at 420 °C. O_2 and O_3 denote here staggered, electrically inactive chains containing two and three oxygen atoms, respectively. The initial oxygen concentration is $[O_i]_\circ = 8 \times 10^{17}$ cm^{-3}. The solid lines denote the simulated results and the symbols the experimental data in Ref. [5].

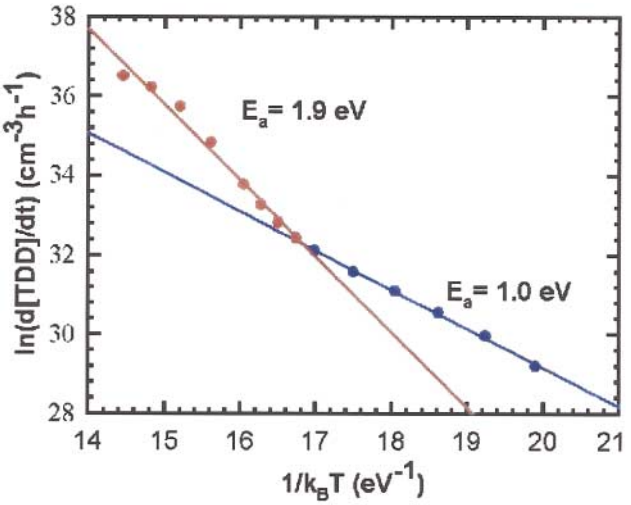

FIG. 5 (color). Arrhenius plot of the calculated formation rate of total TDD's. The simulations are performed for the samples with an initial interstitial oxygen concentration of $[O_i]_\circ = 1.0 \times 10^{18}$ cm^{-3} and $\mu_e = 0.38$ eV.

species (see Refs. [1] and [8]). In fact, we find that the reactions $O_2 + O_n \rightarrow O_{n+2}$ ($n \geq 2$) occur at a negligible rate. This is natural because $[O_i] \geq 1000 \times [O_2]$.

To determine the effective activation energies for the formation of TDD's we use the Arrhenius relation of reaction rate to temperature. The calculated total TDD formation rate is plotted in logarithmic scale as a function of inverse temperature as shown in Fig. 5. The kinetic simulations give an activation energy of 1.0 eV at low temperatures 300–420 °C and 1.9 eV at intermediate temperatures 420–530 °C. These values of 1.0 and 1.9 eV are in close agreement with the experimental values 1.2 eV [9] and 1.7–1.8 eV [9,11,12] at corresponding experimental temperatures, respectively. The activation energy of 1.9 eV results from the involvement of interstitial oxygen O_i with a migration energy of 2.54 eV as well as oxygen chains in the formation of TDD's.

In conclusion, we have introduced a general kinetic model based on the first-principles results to describe the formation kinetics of thermal double donors in silicon. The simulated behaviors agree with a whole host of experiments. The aggregation is found to take place through parallel-consecutive reactions where first fast migrating O_2's, and then fast migrating O_3's and thermal double donors (or the corresponding O chains) capture O_i's.

We thank Professor M. J. Puska and Dr. J.-L. Mozos for many valuable discussions. We acknowledge the generous computing resources of the Center of the Scientific Computing (CSC). This work has been supported by the Academy of Finland (Center of Excellence Program 2000–2005).

[1] *Early Stages of Oxygen Precipitation in Silicon,* edited by R. Jones (Kluwer Academic Publishers, Dordrecht, 1996).
[2] C. A. J. Ammerlaan, in *Properties of Crystalline Silicon,* edited by R. Hull (INSPEC, London, 1999), p. 663.
[3] J. L. Lindström and T. Hallberg, Phys. Rev. Lett. **72**, 2729 (1994).
[4] T. Hallberg and J. L. Lindström, J. Appl. Phys. **79**, 7570 (1996).
[5] D. Åberg, B. G. Svensson, T. Hallberg, and J. L. Lindström, Phys. Rev. B **58**, 12 944 (1998).
[6] M. Pesola, J. von Boehm, and R. M. Nieminen, Phys. Rev. Lett. **82**, 4022 (1999).
[7] H. J. Stein and J. W. Medernach, J. Appl. Phys. **79**, 2337 (1996).
[8] L. I. Murin and V. P. Markevich, in Ref. [1], p. 329.
[9] T. Hallberg and J. L. Lindström, Mater. Sci. Eng. B **36**, 13 (1996).
[10] J. L. Lindström and T. Hallberg, in Ref. [1], p. 41.
[11] M. Claybourn and R. C. Newman, Appl. Phys. Lett. **51**, 2197 (1987).
[12] V. P. Markevich, L. F. Makarenko, and L. I. Murin, Phys. Status Solidi (a) **93**, K173 (1986).
[13] W. Götz, G. Pensl, W. Zulehner, R. C. Newman, and S. A. McQuaid, J. Appl. Phys. **84**, 3561 (1998).
[14] M. Pesola, Y. J. Lee, J. von Boehm, M. Kaukonen, and R. M. Nieminen, Phys. Rev. Lett. **84**, 5343 (2000).
[15] L. C. Snyder, J. W. Corbett, P. Deák, and R. Wu, Mater. Res. Soc. Symp. Proc. **104**, 179 (1988).
[16] S. Pöykkö, M. J. Puska, and R. M. Nieminen, Phys. Rev. B **57**, 12174 (1998).
[17] D. Vanderbilt, Phys. Rev. B **41**, 7892 (1990).
[18] D. R. Hamann, Phys. Rev. B **40**, 2980 (1989).
[19] M. Kaukonen, P. K. Sitch, G. Jungnickel, R. M. Nieminen, S. Pöykkö, D. Porezag, and Th. Frauenheim, Phys. Rev. B **57**, 9965 (1998).
[20] T. R. Waite, Phys. Rev. **107**, 463 (1957).
[21] M. Stavola, J. R. Patel, L. C. Kimmerling, and P. E. Freeland, Appl. Phys. Lett. **42**, 73 (1983).
[22] M. Needels, J. D. Joannopoulos, Y. Bar-Yam, and S. T. Pantelides, Phys. Rev. B **43**, 4208 (1991).
[23] The details of the charge-exchange assisted diffusion will be published elsewhere.
[24] Ya. I. Latushko, L. F. Makarenko, V. P. Markevich, and L. I. Murin, Phys. Status Solidi (a) **93**, K181 (1986).
[25] P. Wagner, and J. Hage, Appl. Phys. A **49**, 123 (1989).